IEEE Access
Multidisciplinary ⋮ Rapid Review ⋮ Open Access Journal

Received July 2, 2021, accepted July 15, 2021, date of publication July 19, 2021, date of current version July 26, 2021.

Digital Object Identifier 10.1109/ACCESS.2021.3098327

Design of a Non-Singular Adaptive Integral-Type Finite Time Tracking Control for Nonlinear Systems With External Disturbances

KHALID A. ALATTAS[1], (Member, IEEE), SALEH MOBAYEN[2], (Senior Member, IEEE), SAMI UD DIN[3], (Member, IEEE), JIHAD H. ASAD[4], AFEF FEKIH[5], (Senior Member, IEEE), WUDHICHAI ASSAWINCHAICHOTE[6], (Member, IEEE), AND MAI THE VU[7]

[1]Department of Computer Science and Artificial Intelligence, College of Computer Science and Engineering, University of Jeddah, Jeddah 23218, Saudi Arabia
[2]Future Technology Research Center, National Yunlin University of Science and Technology, Douliu 64002, Taiwan
[3]Department of Electrical Engineering, Namal Institute Mianwali, Mianwali 42250, Pakistan
[4]Department of Physics, Faculty of Applied Sciences, Palestine Technical University, Tulkarm, Palestine
[5]Department of Electrical and Computer Engineering, University of Louisiana at Lafayette, Lafayette, LA 70504, USA
[6]Department of Electronic and Telecommunication Engineering, Faculty of Engineering, King Mongkut's University of Technology Thonburi, Bangkok 10140, Thailand
[7]School of Intelligent Mechatronics Engineering, Sejong University, Seoul 05006, South Korea

Corresponding authors: Saleh Mobayen (mobayens@yuntech.edu.tw), Wudhichai Assawinchaichote (wudhichai.asa@kmutt.ac.th), and Mai The Vu (maithevu90@sejong.ac.kr)

ABSTRACT This paper proposes an adaptive non-singular fast terminal sliding mode control (FTSMC) with integral surface for the finite time tracking control of nonlinear systems with external disturbances. An appropriate parameter-tuning adaptation law is derived to tackle the disturbances. A new fast terminal sliding scheme with self-tuning algorithm is proposed to synthesize the adaptive non-singular fast integral terminal sliding approach. The proposed approach has the following features: 1) It does not require the derivative of the fractional power terms with respect to time, thereby eschewing the singularity problem typically associated with TSMC; 2) It guarantees the existence of the switching phase under exogenous disturbances with unknown bounds; 3) Because of the integral terms in the sliding surface, the power functions are hidden behind the integrator; 4) It ensures chattering-free dynamics. The effectiveness of the proposed approach is assessed using both a simulation and an experimental study. The obtained results showed that the FTSM control technique guarantees that when the switching surface is reached, tracking errors converge to zero at a fast convergence rate. Additionally, the integral term offers one extra degree-of-freedom and since the time-derivative of fractional power terms is not needed in the controller, the proposed switching surface provides a comprehensive framework for singularity avoidance.

INDEX TERMS Non-singular control, sliding mode control, integral sliding surface, adaptive control, nonlinear system.

I. INTRODUCTION

A. BACKGROUND AND MOTIVATION

Sliding Mode Control (SMC) is a powerful tool for solving the robust stability and tracking problem of nonlinear dynamical systems operating under various kinds of uncertainties and disturbances [1]–[7]. The key advantages of SMC are robustness to parametric uncertainties, low sensitivity to external disturbances, order reduction, fast convergence, and ease of implementation [8]–[11]. Due to these advantages, SMC has been extensively used in applications including robotics, chaotic systems, wind power systems, etc. [12]–[16]. Although SMC guarantees robustness and performance, it suffers from the chattering phenomenon mainly caused by the high frequency switching of the SMC exciting the system's unmolded dynamics [17], [18]. A number of approaches such as the boundary-layer approach via sigmoid and saturation functions [19], disturbance-estimation and observer-based techniques [20], high-order SMC scheme [21], [22], and artificial intelligence (AI) strategies [23] have been proposed in the literature to either reduce or eliminate the chattering phenomena.

An adaptive nonlinear SMC technique with fast chattering-free and non-overshooting responses is developed in [24] for nonlinear multi-input multi-output (MIMO) systems. In [25],

The associate editor coordinating the review of this manuscript and approving it for publication was Shihong Ding.

an adaptive chattering-free SMC approach based on the proportional-integral switching manifold is proposed to stabilize MIMO systems with matched and mismatched uncertainties. In [26], under the assumption that the bound of parameter uncertainties and its first-derivative are unknown, a chattering-free SMC for a perturbed chaotic system is suggested. In [27], a chattering-free adaptive robust SMC is proposed for the synchronization of two chaotic systems with disturbances and unknown uncertainties. In [28], a dynamic output-feedback SMC strategy which eschews the chattering phenomenon and the high-gain control problem is developed for the stabilization of linear MIMO systems with uncertainties. An adaptive fuzzy chattering-free SMC is proposed in [29] for nonlinear single-input single-output (SISO) systems. In [30], a chattering-free robust control scheme based on the adaptive second-order SMC and resonant control laws is suggested for LCL shunt active power filters. In [31], an augmented chattering-free proportional-integral switching surface-based SMC design is proposed of a coalmine power grid with chaotic structure. In [32], an adaptive chattering-free SMC technique is proposed for the precision motion of a piezoelectric nano-positioning system subject to perturbations.

In conventional SMC approaches, the employed switching manifold is often linear and guarantees the asymptotic stabilization of the controlled system and the convergence of the state trajectories to zero in infinite interval. Terminal Sliding Mode (TSM) Control, on the other hand, enables finite time convergence and a smaller steady-state tracking error [33], [34]. However, the singularity problem of TSM leads to unbounded control inputs. Additionally, when the states/tracking errors are far away from zero, TSM shows a slow convergence rate compared to conventional SMC [35], [36]. Therefore, the singularity and chattering problems of TSM method must be properly addressed. The TSM control scheme is actually very sensitive around the equilibrium point and due to the fractional power terms and their negative fractional power derivatives, this method can yield unexpectedly large values leading to the singularity problem.

B. LITERATURE REVIEW

Various non-singular TSM approaches have been investigated in recent years to mitigate singularity problem. A non-singular TSM control method was proposed in [37] for rigid manipulators; however, the adaptation law was not designed in [37]. An adaptive Fast Terminal Sliding Mode (FTSM) method which removes the singular problems of the original TSM is proposed in [38] for an electromechanical actuator system. Parametric uncertainties are approximated in that method [38] using the integration of the filtered states. In [39] and [40], using the non-singular TSM concept, a finite time attitude tracker is designed to drive the angular velocity and attitude tracking errors of a spacecraft to the origin in finite time. However, those techniques considered in [39] and [40] cannot adaptively estimate the bounds of the perturbations. In [41], a modified time-varying non-singular TSM approach is presented for rigid manipulators with perturbations where the system's performance is enhanced by adding a time-varying gain in the sliding manifold. In [42], a passive finite time fault-tolerant controller according to the robust non-singular FTSM is planned for robotic manipulators with actuator faults and parametric uncertainties. An online time-delay estimator-based fault estimation algorithm is presented in [42] to approximate the actuator faults. In [43], a non-singular FTSM is combined with an adaptation technique for the stabilization of an aircraft with varying gravity center. However, the designed method [43] is only valid for a specific nonlinear model. In [44], a non-singular FTSM control method based on the tracker differentiator and extended state observer is proposed for uncertain permanent magnet synchronous motor systems. The approach [44], however, exhibits small chattering dynamics. Xin *et al.* [45] studied the adaptive robust non-singular FTSM control for second-order uncertain systems; however, the designed method of [45] is not presented for high-order dynamic systems. In [46], a robust adaptive gain non-singular TSM approach is provided for a tracker design of formation flying of spacecraft in a framework based on leader-follower approach, but some considerable chattering can be observed in the results of [46]. The theory of [47] studies non-singular adaptive TSM control technique for an attitude tracker design of spacecraft with faults on actuators; but again, the chattering phenomenon is obvious in the presented outcomes. In [48], an adaptive non-singular second-order FTSM controller is planned for n-link robotic manipulators; however, some high-frequency oscillations are experienced in the controller inputs. Nevertheless, to the best of our knowledge, the non-singular switching manifolds had been designed via a power function which is a ratio of odd positive integers. By employing an integral term in the proposed sliding surface, there is no restriction on the exponents and the power functions are 'hidden' behind the integrator in the sliding surface.

C. CONTRIBUTIONS

This paper proposes an adaptive non-singular fast terminal sliding mode control (FTSMC) with integral surface for the finite time tracking control of nonlinear systems with external disturbances. Its main contributions are as follows:

- A non-singular FTSM strategy and proportional-integral switching surface that guarantees the finite time convergence of the switching surfaces to zero with fast convergence rate.
- A design that does not require the time-derivative of the fractional power terms in the controller, thereby avoiding the singularity problem.
- By using a bipolar sigmoid function with tunable gains instead of a signum function, an appropriate adaptation law is derived to tackle the external disturbances without any knowledge about the bounds of the perturbations.
- A new adaptation law to mitigate the chattering problem.

D. PAPER ORGANIZATION

The remainder of the paper is organized as follows. Section 2 formulates the control problem and describes the dynamics of the disturbed nonlinear system under consideration. The design process for the adaptive non-singular fast integral terminal sliding controller technique is provided in Section 3. Simulation studies and experimental results are presented in Section 4 to validate the efficiency of proposed approach. Lastly, some concluding remarks are presented in Section 5.

II. PROBLEM FORMULATION

Consider the nonlinear system with external disturbances defined by:

$$\dot{x}_1(t)=x_2(t), \quad \dot{x}_2(t)=f(x,t)+b(x,t)u(t)+d(x,t), \tag{1}$$

where time $t \geq 0$, $x = [x_1, x_2]^T$, $x_1(t) \in \mathbb{R}$ and $x_2(t) \in \mathbb{R}$ denote the states, $u(t) \in \mathbb{R}$ is control input, $b(x,t) \in \mathbb{R}$, $(b(x,t) \neq 0)$ and $f(x,t) \in \mathbb{R}$ are two bounded known smooth and nonlinear functions, and $d(x,t) \in \mathbb{R}$ is a nonlinear function representing the uncertainties and disturbances, and is assumed to fulfill $|d(x,t)| \leq D$, where D denotes a known constant scalar. The nonlinear dynamic system (1) is assumed to track the references $x_{1d}(t) \in \mathbb{R}$ and $x_{2d}(t) \in \mathbb{R}$, where $x_{2d}(t) = \dot{x}_{1d}(t)$, and $x_{2d}(t)$ denotes a time-differentiable function. One can consider the tracking errors as:

$$\begin{bmatrix} e_1(t) \\ \dot{e}_1(t) \end{bmatrix} = \begin{bmatrix} x_1(t) - x_{1d}(t) \\ x_2(t) - x_{2d}(t) \end{bmatrix}, \tag{2}$$

with $\dot{e}_1(t) = e_2(t)$. Considering (1) and (2), one obtains:

$$\dot{e}_2(t) = -\dot{x}_{2d}(t) + f(x,t) + b(x,t)u(t) + d(x,t) \tag{3}$$

Our main objectives is to design a robust SMC-based tracking control approach that: 1) guarantees the convergence of the states of (1) to the desired trajectory; 2) ensures that when the switching surface is reached, the tracking errors converge to zero at a fast convergence rate; 3) warrants the existence of the switching phase in the presence of exogenous disturbances d(x, t) with unknown bounds; 4) properly mitigates the singularity and chattering problems.

III. CONTROLLER DESIGN

Define the following switching surface for the nonlinear system (1):

$$s(t) = e_2(t) + \int_0^t \left(c_1 S_1(e_1(\tau)) + c_2 S_2(e_2(\tau))\right) d\tau, \tag{4}$$

where $S_1(e_1(\tau))$ and $S_2(e_2(\tau))$ are specified by

$$S_i(e_i(t)) = \begin{cases} sgn(e_i(t))\,|e_i(t)|^{\gamma_i}, & if \ \ |e_i(t)| \leq \varepsilon_i \\ \varepsilon_i^{\gamma_i-\rho_i} sgn(e_i(t))\,|e_i(t)|^{\rho_i}, & if \ \ |e_i(t)| > \varepsilon_i \end{cases} \tag{5}$$

for $i = 1, 2$, where the time t is bounded, and the constant coefficients γ_i, ρ_i, c_i and ε_i satisfy $\gamma_1 = \frac{\gamma_2}{2-\gamma_2}$, $0 < \gamma_2 < 1$, $\rho_1, \rho_2 \geq 1$, $1 > \varepsilon_1, \varepsilon_2 > 0$ and $c_1, c_2 > 0$.

Remark 1: The condition (5) has a structure like a boundary layer, which is an extension of the sliding function described in [49]. For $|e_i(t)| \leq \varepsilon_i$, the term $S_i(t)$ is similar to a fractional power term. If $|e_i(t)| > \varepsilon_i$, then $|e_i(t)|^{\rho_i} > \varepsilon_i^{\rho_i}$ and if $|e_i(t)| \leq \varepsilon_i$, then $|e_i(t)|^{\gamma_i} \leq \varepsilon_i^{\gamma_i}$. As a result, one obtains $\varepsilon_i^{\gamma_i-\rho_i}|e_i(t)|^{\rho_i} > \varepsilon_i^{\gamma_i-\rho_i}\varepsilon_i^{\rho_i} = \varepsilon_i^{\gamma_i} \geq |e_i(t)|^{\gamma_i}$ and $\left|\varepsilon_i^{\gamma_i-\rho_i} sgn(e_i(t))\right| |e_i(t)|^{\rho_i} > |sgn(e_i(t))|\,|e_i(t)|^{\gamma_i}$. Hence, when $|e_i(t)| > \varepsilon_i$, the absolute value of the term $S_i(t)$ is bigger than the fractional power term of $|e_i(t)| \leq \varepsilon_i$. Then, a fast convergence rate in both cases is achieved by increasing the magnitude of the parameters ε_i and ρ_i.

Theorem 1: Consider the second-order nonlinear dynamic system (1) and the switching surface (4). Assume that the equivalent controller is proposed as:

$$u_{eq}(t) = -b(x,t)^{-1}\{f(x,t) + c_1 S_1(e_1(t)) + c_2 S_2(e_2(t)) - \dot{x}_{2d}(t) + d(x,t)\}. \tag{6}$$

Then, the state trajectories of (1) converge to the desired trajectory along the sliding mode $s(t) = 0$.

Proof: The time-derivative of the switching curve (4) is set equal to zero as follows:

$$\dot{s}(t) = \dot{e}_2(t) + c_1 S_1(e_1(t)) + c_2 S_2(e_2(t)) = 0. \tag{7}$$

Substituting the equivalent control signal (6) into (3), yields the equivalent dynamics:

$$\dot{e}_1(t) = e_2(t), \quad \dot{e}_2(t) = -c_1 S_1(e_1(t)) - c_2 S_2(e_2(t)). \tag{8}$$

Consider the positive-definite Lyapunov function:

$$V_1(e_1(t), e_2(t)) = \int_0^{e_1(t)} c_1 S_1(e_1(\tau))\, de_1(\tau) + \frac{1}{2} e_2^2(t), \tag{9}$$

Differentiating $V_1(t)$ along the trajectories of system (8) gives:

$$\begin{aligned} \dot{V}_1(t) &= \begin{bmatrix} c_1 S_1(t) & e_2(t) \end{bmatrix} \begin{bmatrix} \dot{e}_1(t) \\ \dot{e}_2(t) \end{bmatrix} \\ &= c_1 S_1(t) e_2(t) - c_1 S_1(t) e_2(t) - c_2 S_2(t) e_2(t) \\ &= -c_2 S_2(t) e_2(t) \leq 0. \end{aligned} \tag{10}$$

Using Lasalle's invariance theorem [50], the set $\{(e_1(t), e_2(t)) : \dot{V}_1(t) = 0\}$ involves $e_2(t) = 0$, and the invariant set inside $e_2(t) = 0$ is $e_1(t) = e_2(t) = 0$. Hence, the asymptotic convergence of the errors to zero is satisfied. It is obvious that if $|e_2(t)| > \varepsilon_2$, then $\dot{V}_1(t) < 0$, and therefore $|e_2(t)|$ is reduced. The tracking errors converge to $\Omega = \{(e_1(t), e_2(t)) : |e_1(t)| \leq \varepsilon_1, |e_2(t)| \leq \varepsilon_2\}$.

When $(e_1(t), e_2(t)) \in \Omega$, according to the definition of $S_i(t)$, $i = 1, 2$ in (5), the system (8) is written as

$$\begin{aligned} &\dot{e}_1(t) = e_2(t), \\ &\dot{e}_2(t) = -c_1 sgn(e_1(t))\,|e_1(t)|^{\gamma_1} - c_2 sgn(e_2(t))\,|e_2(t)|^{\gamma_2}, \end{aligned} \tag{11}$$

where substituting (11) into (10), one obtains

$$\dot{V}_1(t) = -c_2\,|e_2(t)|^{\gamma_2+1} \leq 0. \tag{12}$$

Therefore, the error dynamic system (8) converges to the origin from any initial condition. □

Remark 2: It should be stated that the design of equivalent controller (6) is inspired by the work of [51]. However, that paper considered a stabilization control problem whereas here we consider a tracking control procedure and the term $\dot{x}_{2d}(t)$ is considered in the equivalent control law (6).

Theorem 2: Consider the disturbed nonlinear second-order dynamics (1) and the switching surface (4). Assume that the controller is described as

$$u(t) = -b(x,t)^{-1}\{f(x,t) - \dot{x}_{2d}(t) + c_1 S_1(e_1(t)) + \gamma s(t) + c_2 S_2(e_2(t)) + \kappa sgn(s(t))\,|s(t)|^{\eta} + \chi\, sgn(s(t))\}, \tag{13}$$

where κ and γ are two arbitrary positive scalars and χ is a constant which fulfils $\chi \geq D$. Then, the tracking purpose of a reference signal $x_d(t)$ is satisfied and the switching surface $s(t)$ converges to the origin within a finite time.

Proof: Construct the Lyapunov function as:

$$V_2(s(t)) = 0.5 s(t)^2. \tag{14}$$

Differentiating the Lyapunov function along the trajectory of (3) and (4), it follows:

$$\dot{V}_2(t) = s(t)[d(x,t) + b(x,t)u(t) + f(x,t) - \dot{x}_{2d}(t) + c_1 S_1(e_1(t)) + c_2 S_2(e_2(t))]. \tag{15}$$

Substituting (13) into (15), one finds

$$\begin{aligned}
\dot{V}_2(t) &= s(t)\Big[b(x,t)\Big(-b(x,t)^{-1}\{f(x,t) - \dot{x}_{2d} + c_1 S_1(t) \\
&\quad + \kappa\,|s(t)|^{\eta} sgn(s) + c_2 S_2(t) + \gamma s(t) + \chi\, sgn(s)\}\Big) \\
&\quad + f(x,t) + d(x,t) - \dot{x}_{2d}(t) + c_1 S_1(t) + c_2 S_2(t)\Big] \\
&= s(t)\left[-\kappa\,|s(t)|^{\eta} sgn(s(t)) - \chi\, sgn(s(t)) + d(x,t) - \gamma s(t)\right] \\
&\leq -\gamma\,|s(t)|^2 - \kappa\,|s(t)|^{\eta+1} - \chi\,|s(t)| + |d(x,t)|\,|s(t)| \\
&\leq -\kappa\,|s(t)|^{\eta+1} - \gamma\,|s(t)|^2 + \{D - \chi\}\,|s(t)| \\
&\leq -\gamma\,|s(t)|^2 - \kappa\,|s(t)|^{\eta+1} \\
&= -\Omega_1 V_2(t) - \Omega_2 V_2(t)^{\bar{\eta}}
\end{aligned} \tag{16}$$

where $\Omega_1 = 2\gamma > 0$, $\Omega_2 = 2^{\bar{\eta}}\kappa > 0$ and $\bar{\eta} = 0.5(\eta + 1) < 1$. Thus, in relation to the finite time stability theory, the manifold $s(t)$ converges to zero and the tracking errors approach to the origin in a finite time. □

In practice, the upper bound of $d(x,t)$ is unknown and the consequent determination of χ is hard. In the next theorem, an adaptation method is planned to approximate the disturbances unknown bounds.

Theorem 3: Consider the nonlinear system (1) and the sliding surface (4). Assume that the bound χ on the disturbance term $d(x,t)$ is unknown, where χ is an unknown (positive) scalar. Then, using the adaptive controller as:

$$\begin{aligned}
u(t) &= -b(x,t)^{-1}\{f(x,t) - \dot{x}_{2d}(t) + c_1 S_1(e_1(t)) \\
&\quad + \gamma s(t) + c_2 S_2(e_2(t)) + \kappa sgn(s(t))\,|s(t)|^{\eta} \\
&\quad + \hat{\chi}(t) sgn(s(t))\},
\end{aligned} \tag{17}$$

$$\dot{\hat{\chi}}(t) = \psi\,|s(t)|, \tag{18}$$

where ψ is a positive scalar, the switching surface $s(t)$ and the tracking errors converge to the origin.

Proof: Define the following Lyapunov function:

$$V_3(s(t), \tilde{\chi}) = 0.5\left(s(t)^2 + \mu\tilde{\chi}(t)^2\right), \tag{19}$$

where $\tilde{\chi}(t) = \hat{\chi}(t) - \chi$ and μ is a positive scalar satisfying $\mu < \psi^{-1}$.

Differentiating (19) along the trajectory of (1), and using (7), yields:

$$\begin{aligned}
\dot{V}_3(t) &= s(t)\left[\dot{e}_2 + c_1 S_1(e_1(t)) + c_2 S_2(e_2(t))\right] \\
&\quad + \mu\psi\left(\hat{\chi}(t) - \chi\right)|s(t)| \\
&= s(t)[f(x,t) + d(x,t) - \dot{x}_{2d}(t) + b(x,t)u(t) \\
&\quad + c_1 S_1(e_1(t)) + c_2 S_2(e_2(t))] \\
&\quad + \mu\psi\left(\hat{\chi}(t) - \chi\right)|s(t)|,
\end{aligned} \tag{20}$$

where substituting (17) into (20) gives

$$\begin{aligned}
\dot{V}_3(t) &= s(t)\,(f(x,t) + d(x,t) - \dot{x}_{2d}(t) + c_1 S_1(e_1(t)) \\
&\quad + c_2 S_2(e_2(t)) \\
&\quad - f(x,t) + \dot{x}_{2d}(t) - c_1 S_1(e_1(t)) \\
&\quad - c_2 S_2(e_2(t)) - \gamma s(t) - \kappa\,|s(t)|^{\eta} sgn(s(t)) \\
&\quad - \hat{\chi}(t) sgn(s(t))) + \mu\psi\left(\hat{\chi}(t) - \chi\right)|s(t)| \\
&= s(t)\left(-\kappa\,|s(t)|^{\eta} sgn(s(t)) - \gamma s(t) - \hat{\chi}(t) sgn(s(t))\right. \\
&\quad \left. + d(x,t)\right) + \mu\psi\left(\hat{\chi}(t) - \chi\right)|s(t)| \\
&\leq -\gamma\,|s(t)|^2 - \kappa\,|s(t)|^{\eta+1} - \hat{\chi}(t)\,|s(t)| \\
&\quad + |d(x,t)|\,|s(t)| + \mu\psi\left(\hat{\chi}(t) - \chi\right)|s(t)| \\
&= -\kappa\,|s(t)|^{\eta+1} - \gamma\,|s(t)|^2 - \hat{\chi}(t)\,|s(t)| \\
&\quad + |d(x,t)|\,|s(t)| \\
&\quad + \mu\psi\left(\hat{\chi}(t) - \chi\right)|s(t)| + \chi\,|s(t)| - \chi\,|s(t)| \\
&= -\gamma\,|s(t)|^2 - (\chi - |d(x,t)|)\,|s(t)| - \kappa\,|s(t)|^{\eta+1} \\
&\quad - (1 - \mu\psi)\left(\hat{\chi}(t) - \chi\right)|s(t)|.
\end{aligned} \tag{21}$$

Since $\chi > |d(x,t)|$ and $\mu < \psi^{-1}$, we can re-write (21) as:

$$\begin{aligned}
\dot{V}_3(t) &\leq -\kappa\,|s(t)|^{\eta+1} - \gamma\,|s(t)|^2 - \sqrt{2}\,(\chi - |d(x,t)|) \\
&\quad \times \frac{|s(t)|}{\sqrt{2}} - \sqrt{2/\mu}\,(1 - \mu\psi)\,\frac{\tilde{\chi}(t)}{\sqrt{2/\mu}}\,|s(t)| \\
&\leq -\kappa\,|s(t)|^{\eta+1} - \gamma\,|s(t)|^2 \\
&\quad - \min\left\{\sqrt{2}\,(\chi - |d(x,t)|)\,,\right. \\
&\quad \left. \times \sqrt{2/\mu}\,(1 - \mu\psi)\,|s(t)|\right\}\left(\frac{|s(t)|}{\sqrt{2}} + \frac{|\tilde{\chi}(t)|}{\sqrt{2/\mu}}\right) \\
&\leq -\Pi\left(\frac{|s(t)|}{\sqrt{2}} + \frac{|\tilde{\chi}(t)|}{\sqrt{2/\mu}}\right),
\end{aligned} \tag{22}$$

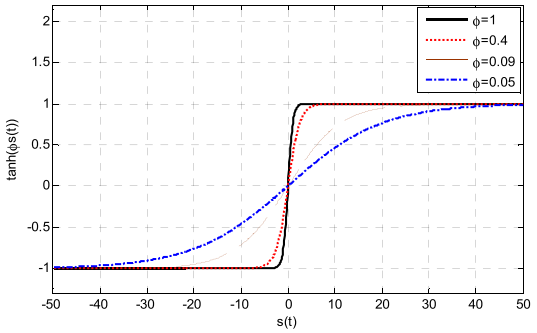

FIGURE 1. Function tanh(with different values of $\hat{\phi}$).

where $\Pi = \min\left\{\sqrt{2}\left(\chi - |d(x,t)|\right), \sqrt{2/\mu}\left(1 - \mu\psi\right)|s(t)|\right\} > 0$. Now,considering the fact that:

$$\left(\frac{|s(t)|}{\sqrt{2}} + \frac{|\tilde{\chi}(t)|}{\sqrt{2/\mu}}\right) = \sqrt{\frac{s(t)^2}{2} + \frac{\tilde{\chi}(t)^2}{(2/\mu)} + \sqrt{\mu}\,|s(t)|\,\tilde{\chi}(t)} \geq \sqrt{\frac{s(t)^2}{2} + \frac{\tilde{\chi}(t)^2}{(2/\mu)}} = V_3(t)^{\frac{1}{2}}, \quad (23)$$

where the last term in (22) becomes less than $-\Pi V_3(t)^{\frac{1}{2}}$, it follows that

$$\dot{V}_3(t) \leq -\Pi V_3(t)^{\frac{1}{2}}. \quad (24)$$

Then, using the adaptive tuning controller (17), the condition $s(t) = 0$ is assured and the states of (1) converge to the desired trajectory. □

Note that the discontinuous sign function proposed in controller (17) causes the chattering phenomenon and results in unwanted responses in the controlled dynamics. Hence, the function *sgn* in (17) is replaced by a continuous hyperbolic tangent function *tanh* with adaptive law to enable the modification of the steepness and amplitude of the control law. As it is displayed in FIGURE 1, the steepness of the hyperbolic tangent function governs how it approximates the sign function. That is, if the steepness constant increases, the obtained function will approach the sign function thereby giving rise to the chattering problem. However, if the steepness and the gain of *tanh* is decreased, then we have chattering-free dynamics. Therefore, the adaptive chattering-free continuous controller is defined by:

$$\begin{aligned} u(t) = & -b(x,t)^{-1} f(x,t) - \dot{x}_{2d} + c_1 S_1(e_1(t)) \\ & + c_2 S_2(e_2(t)) + \gamma s(t) + \kappa sgn(s(t))\,|s(t)|^{\eta} \\ & + \hat{\chi}(t) tanh(\hat{\varphi}(t)s(t))\}, \end{aligned} \quad (25)$$

where $\hat{\varphi}(t)$ is the adaptive steepness coefficient of *tanh* which is considered as

$$tanh(\hat{\varphi}(t)s(t)) = \frac{exp(\hat{\varphi}(t)s(t)) - exp(-\hat{\varphi}(t)s(t))}{exp(\hat{\varphi}(t)s(t)) + exp(-\hat{\varphi}(t)s(t))} \quad (26)$$

where the constant control parameters are arbitrary positive scalars which are selected by trial and error approach.

Theorem 4: Consider the dynamics (1) and the switching manifold (4). If the controller signal is chosen as (25) and the adaptation rules are designed as

$$\begin{aligned} \dot{\hat{\varphi}}(t) = & \; 0.25\alpha b(x,t)\left(exp(-\hat{\varphi}(t)s(t)) + exp(\hat{\varphi}(t)s(t))\right)^2 \\ & \times \hat{\chi}(t)^{-1}\frac{\dot{s}(t)}{s(t)} sgn\left(\frac{\partial \dot{s}(t)}{\partial u(t)}\right) \end{aligned} \quad (27)$$

$$\begin{aligned} \dot{\hat{\chi}}(t) = & \; \beta b(x,t)\frac{exp(-\hat{\varphi}(t)s(t)) + exp(\hat{\varphi}(t)s(t))}{exp(\hat{\varphi}(t)s(t)) - exp(-\hat{\varphi}(t)s(t))} \\ & \times \dot{s}(t)^{\eta} sgn\left(\frac{\partial \dot{s}(t)}{\partial u(t)}\right) \end{aligned} \quad (28)$$

where $\alpha, \beta > 0$, as a result, the error states are forced to switching curve and the convergence to zero in a finite time is obtained.

Proof: Construct the positive-definite Lyapunov function as

$$V_4(s(t)) = 0.5\dot{s}(t)^2, \quad (29)$$

where differentiating $V_4(t)$ results in

$$\dot{V}_4(t) = \frac{\partial V_4(s(t))}{\partial \dot{s}(t)}\frac{\partial \dot{s}(t)}{\partial u(t)}\left(\frac{\partial u(t)}{\partial \hat{\chi}(t)}\frac{\partial \hat{\chi}(t)}{\partial t} + \frac{\partial u(t)}{\partial \hat{\varphi}(t)}\frac{\partial \hat{\varphi}(t)}{\partial t}\right). \quad (30)$$

Now, manipulating the above equation, we get:

$$\begin{aligned} \dot{V}_4(t) = & \frac{\partial V_4}{\partial \dot{s}(t)}\frac{\partial \dot{s}(t)}{\partial u(t)}\frac{\partial u(t)}{\partial \hat{\chi}(t)}\frac{\partial \hat{\chi}(t)}{\partial t} \\ & +, \frac{\partial V_4}{\partial \dot{s}(t)}\frac{\partial \dot{s}(t)}{\partial u(t)}\frac{\partial u(t)}{\partial \hat{\varphi}(t)}\frac{\partial \hat{\varphi}(t)}{\partial t} \\ = & \; \dot{s}(t)\frac{\partial \dot{s}(t)}{\partial u(t)}\frac{\partial}{\partial \hat{\chi}(t)}\Big(-b(x,t)^{-1}\{f(x,t) - \dot{x}_{2d} \\ & + c_1 S_1(e_1(t)) + c_2 S_2(e_2(t)) \\ & + \kappa\,|s(t)|^{\eta}\,sgn(s(t)) + \gamma s(t) \\ & + \hat{\chi}\frac{exp(s(t)\hat{\varphi}(t)) - exp(-s(t)\hat{\varphi}(t))}{exp(s(t)\hat{\varphi}(t)) + exp(-s(t)\hat{\varphi}(t))}\Big\}\Big)\dot{\hat{\chi}}(t) \\ & + \dot{s}(t)\frac{\partial \dot{s}(t)}{\partial u(t)}\frac{\partial}{\partial \hat{\varphi}(t)}\Big(-b(x,t)^{-1}\{f(x,t) - \dot{x}_{2d}(t) \\ & + c_1 S_1(e_1(t)) + c_2 S_2(e_2(t)) + \gamma s(t) \\ & + \kappa\,|s(t)|^{\eta}\,sgn(s(t)) \\ & + \hat{\chi}(t)\frac{exp(s(t)\hat{\varphi}(t)) - exp(-s(t)\hat{\varphi}(t))}{exp(s(t)\hat{\varphi}(t)) + exp(-s(t)\hat{\varphi}(t))}\Big\}\Big)\dot{\hat{\varphi}}(t) \end{aligned} \quad (31)$$

where substituting the differentiation of $u(t)$ with respect to $\hat{\chi}(t)$ and $\hat{\varphi}(t)$ into $\dot{V}_4(t)$, it gives

$$\begin{aligned} \dot{V}_4(t) = & -\dot{s}(t)\frac{\partial \dot{s}(t)}{\partial u(t)} b(x,t)^{-1} \\ & \times \left(\hat{\chi}(t)\frac{4s(t)}{\left(exp(-\hat{\varphi}(t)s) + exp(\hat{\varphi}(t)s)\right)^2}\dot{\hat{\varphi}}(t)\right. \\ & \left. + \frac{exp(\hat{\varphi}(t)s(t)) - exp(-\hat{\varphi}(t)s(t))}{exp(-\hat{\varphi}(t)s(t)) + exp(\hat{\varphi}(t)s(t))}\dot{\hat{\chi}}(t)\right). \end{aligned} \quad (32)$$

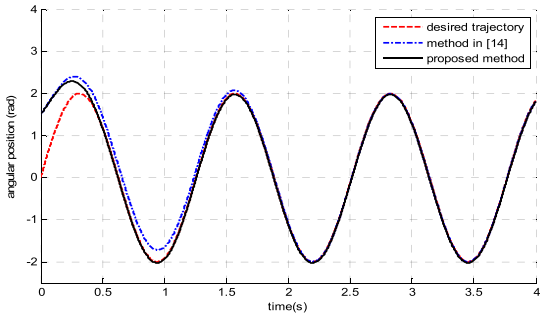

FIGURE 2. Time trajectory of $x_1(t)$, $t \geq 0$.

Finally, using the adaptation laws (27) and (28) in the above equation yields

$$\begin{aligned}\dot{V}_4(t) &= -\alpha \dot{s}(t)^2 \left|\frac{\partial \dot{s}(t)}{\partial u(t)}\right| - \beta \dot{s}(t)^{\eta+1} \left|\frac{\partial \dot{s}(t)}{\partial u(t)}\right| \\ &\leq -\Lambda_1 V_4(t) - \Lambda_2 V_4(t)^{\bar{\eta}} \end{aligned} \tag{33}$$

where $\bar{\eta} = \frac{\eta+1}{2}$, $\Lambda_1 \leq 2\alpha \left|\frac{\partial \dot{s}(t)}{\partial u(t)}\right|$ and $\Lambda_2 \leq 2^{\bar{\eta}} \beta \left|\frac{\partial \dot{s}(t)}{\partial u(t)}\right|$. This finalizes the proof. □

Remark 3: In order to completely eliminate the chattering problem resulting from the discontinuous sign function (sgn($s(t)$)), the control signal (25) and the adaptation tuning equations (27)-(28) are adapted via a hyperbolic tangent. Hence, the controller input and adaptation tuning equations are obtained as:

$$\begin{aligned} u(t) = &-b(x,t)^{-1} f(x,t) - \dot{x}_{2d}(t) + c_1 S_1(e_1(t)) \\ &+ c_2 S_2(e_2(t)) + \gamma s(t) + \kappa tanh(\Im s(t))\, |s(t)|^{\eta} \\ &+ \hat{\chi}(t) tanh(\hat{\varphi}(t) s(t))\}, \end{aligned} \tag{34}$$

and

$$\begin{aligned} \dot{\hat{\varphi}}(t) = &\, 0.25 \alpha b(x,t) \left(exp(s(t)\hat{\varphi})\right. \\ &+ exp(-s(t)\hat{\varphi}))^2 \hat{\chi}(t)^{-1} \dot{s}(t) s(t)^{-1} tanh\left(\Im \frac{\partial \dot{s}}{\partial u}\right), \end{aligned} \tag{35}$$

$$\begin{aligned} \dot{\hat{\chi}}(t) = &\, \beta b(x,t) \frac{exp(-\hat{\varphi} s(t)) + exp(s(t)\hat{\varphi})}{exp(s(t)\hat{\varphi}) - exp(-s(t)\hat{\varphi})} \\ &\times \dot{s}(t)^{\eta} tanh\left(\Im \frac{\partial \dot{s}(t)}{\partial u(t)}\right), \end{aligned} \tag{36}$$

where $\Im$ is the steepness constant of the hyperbolic tangent. Note selecting a $\Im$ to be very small can lead to steady-state errors, whereas assigning too large of a value for $\Im$ can give rise to the chattering problem. Thus, the value of $\Im$ is required to be chosen suitably based on each specific system.

Considering the tracking control problem, the performance indices are presented as the objective functions which will be used in the next section:

(I) Integral of Absolute of Error (IAE): $J_i^1(t) = \int_0^t |e_i(\tau)|\, d\tau, i = 1, \ldots, n,$

(II) Integral of Time-multiplied Absolute of Error (ITAE): $J_i^2(t) = \int_0^t \tau\, |e_i(\tau)|\, d\tau, i = 1, \ldots, n,$

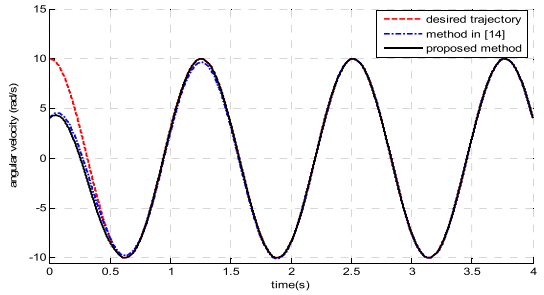

FIGURE 3. Time history of $x_2(t)$, $t \geq 0$.

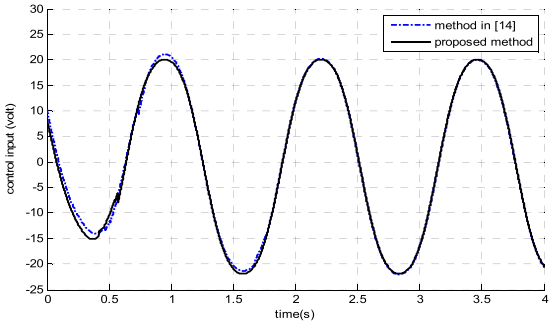

FIGURE 4. The control signal u(t), $t \geq 0$ (Eq. (34)).

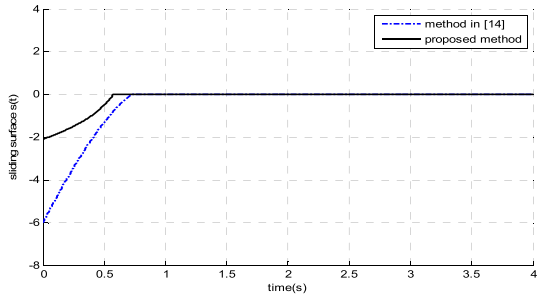

FIGURE 5. Sliding surface s(t), $t \geq 0$ (Eq.(4)).

(III) Integral of Square Value of control signal (ISV): $J^3(t) = \int_0^t u(\tau)^2 d\tau$.

IV. SIMULATION AND EXPERIMENTAL RESULTS

To assess the performance of the proposed approach, we carry out a simulation and experimental study. Additionally, for comparison purposes, we consider the approach proposed in [14].

A. EXAMPLE 1: VAN DER POL CIRCUIT SYSTEM

Van der Pol (VDP) circuits are often considered in analysing nonlinear systems, to highlight many phenomena including stability, limit-cycle, relaxation oscillation, and Hopf-bifurcation. This system is extremely nonlinear and displays both stable and unstable limit cycles. The VDP oscillator is introduced by the equation [52]:

$$\ddot{x}(t) + \mu_0 (x(t)^2 - 1)\dot{x}(t) + x(t) = 0, \tag{37}$$

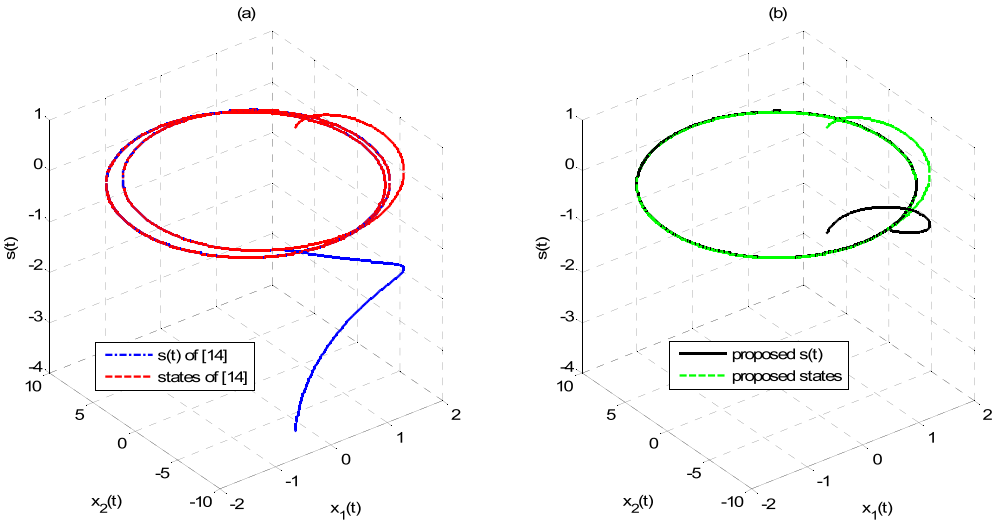

FIGURE 6. Phase plot of the states and sliding surfaces; (a) method of [14], (b) proposed method.

where μ_0 is a positive constant. Eq. (37) is a simple harmonic oscillator, with the nonlinear damping $\mu_0(x(t)^2 - 1)\dot{x}(t)$. When $|x(t)| > 1$, the nonlinear term causes large amplitude to decay. When $|x(t)| < 1$, the nonlinear damping term increases. Consequently, this circuit reaches a self-sustained oscillation and has a unique stable limit cycle. The dynamic equation of a forced VDP circuit is presented as [53]:

$$\ddot{x}(t) + 3(x(t)^2 - 1)\dot{x}(t) + 2x(t) = u(t) + d(t), \qquad (38)$$

where $x(t)$ denotes the system state; $u(t)$ represents the control signal, and $d(t)$ indicates the external disturbances. Eq. (38) can be written in state-space form as [54]:

$$\begin{aligned} \dot{x}_1(t) &= x_2(t) \\ \dot{x}_2(t) &= -2x_1(t) + 3(1 - x_1(t)^2)x_2(t) + u(t) + d(t), \end{aligned} \qquad (39)$$

where $x_1(t)$, $x_2(t)$ are the state variables. The disturbance term is considered as $d(t) = 0.3\,sin(0.2\pi\sqrt{t+1}) + 0.2\,sin(0.1\pi t)$. The system states must track the desired trajectories $x_{1d}(t) = 2\,sin(5t)$ and $x_{2d}(t) = 10\,cos(5t)$. The initial condition is selected as $x(0) = \left[\,1.5,\ 4\,\right]^T$. The controller parameters are determined by trial and error and are obtained as follows: $\kappa = 5$, $\gamma = \eta = 0.3$, $\psi = 0.7$, $\gamma_1 = \frac{1}{3}$, $\gamma_2 = 0.5$, $\varepsilon_1 = 0.05$, $\varepsilon_2 = 0.08$, $\rho_1 = 1.1$, $\rho_2 = 1.05$, $c_1 = 0.5$, $c_2 = 1.2$.

The time histories of the system state variables x_1 and x_2 are displayed in FIGURE 2 and FIGURE 3. It can be seen from these two figures that the suggested approach offers more accurate and much fast transient response than the approach in [14]. The comparison of the control signals is exhibited in FIGURE 4 which indicates that the planned controller yields superior vibration control. The time histories of the switching surfaces are shown in FIGURE 5. Evidently, the quick convergence of the proposed switching curve to zero in comparison with the switching surface of [14] can be observed. FIGURE 6 shows the phase plots of the states

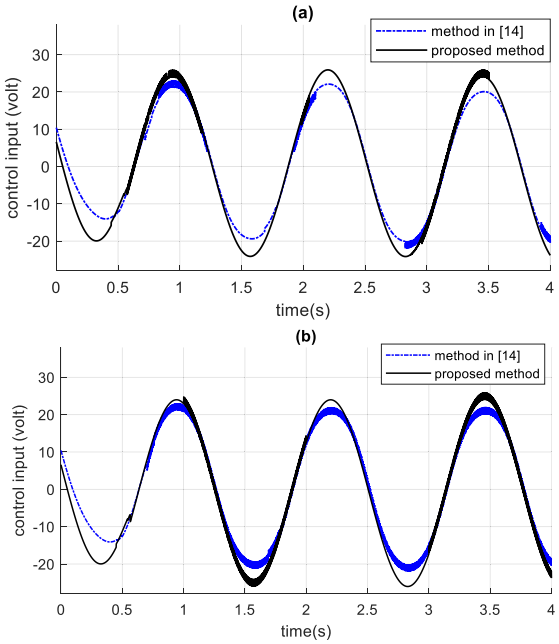

FIGURE 7. Control inputs in the presence of (a) triangle wave disturbance, (b) square wave disturbance.

and sliding surfaces, which demonstrates that the proposed sliding surface and the system states have faster transient response compared to the method of [14]. Table 1 presents the IAE, ITAE and ISV numerical results. Using the proposed control technique, the performance indices of tracking errors and control signals are smaller compared to results of the technique of [14]. This result demonstrates the enhanced tracking performance of the proposed technique over the other existing ones. In summary, the simulation results on the VDP circuit validate the efficiency and usefulness of the newly introduced control scheme.

Two other simulations are conducted to examine the robustness of the suggested control method to different

TABLE 1. Performance indices (IAE, ITAE, ISV) of the VDP circuit system.

	IAE		ITAE		ISV
	e_1	e_2	e_1	e_2	
proposed method	5.2961	24.843	10.032	52.452	34.123
method in [14]	5.3605	25.085	10.122	52.657	34.329

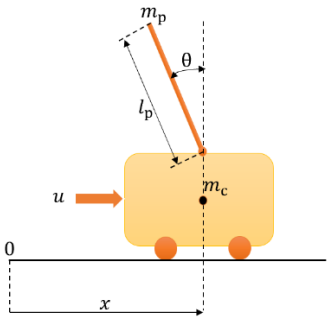

FIGURE 8. Mechanical model of inverted pendulum.

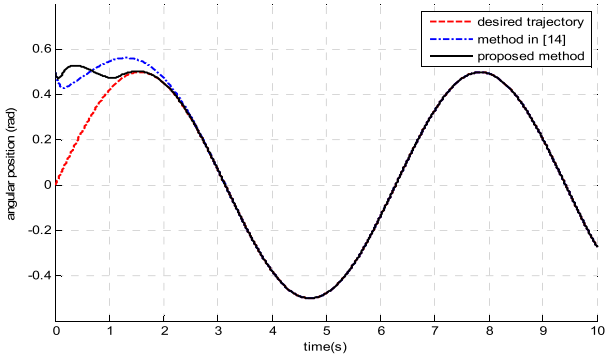

FIGURE 9. Angular position.

external disturbances. To that end, the external disturbances are set to triangle and square waveforms with $d(t) = \begin{cases} -0.5\,(t-1)\,, 0 \le t < 2 \\ 0.5\,(t-3)\,, 2 \le t < 4 \end{cases}$ and $d(t) = \begin{cases} 0.5, 0 \le t < 1 \\ -0.5, 1 \le t < 2 \end{cases}$, respectively. The simulations are rerun without retuning the controller gains. In both cases, the simulation results of the tracking performance and sliding surfaces are nearly identical to the ones for the sinusoidal disturbance $d(t) = 0.3\,sin(0.2\pi\sqrt{t+1}) + 0.2\,sin(0.1\pi t)$, and thus are not reproduced here. Time responses of the control inputs are given in FIGURE 7, which shows some chattering issues in the new conditions.

B. EXAMPLE 2: INVERTED PENDULUM SYSTEM

The inverted pendulum is a famous test system for assessing control strategies [55], [56]. This system is widely used for educational goals, and belongs to the under-actuated mechanical systems. It also has specific various real-life usages such as robotics, position control, aerospace vehicles control, etc. [55]. The main control objective is to balance or stabilize the pendulum in the inverted position. The schematic representation of the inverted pendulum system is shown

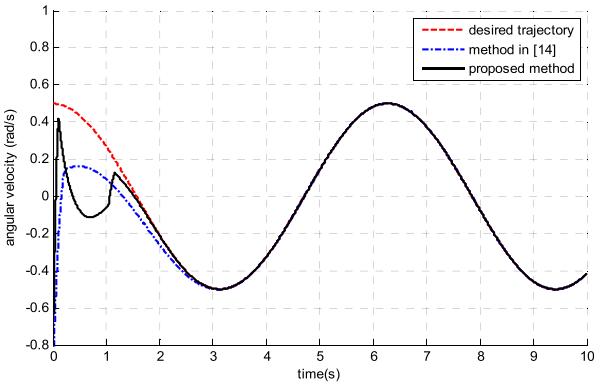

FIGURE 10. Angular velocity.

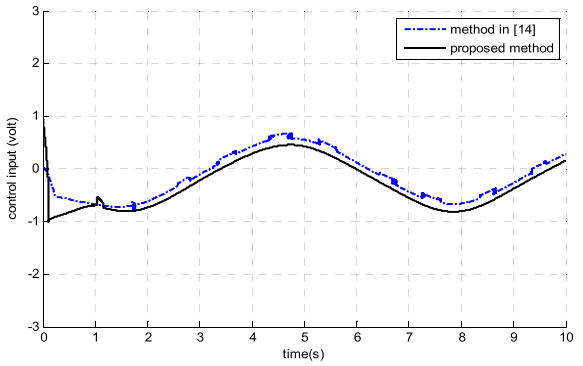

FIGURE 11. Control input.

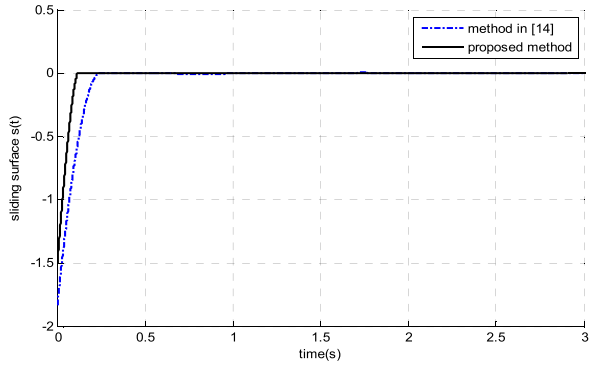

FIGURE 12. Sliding surface s(t).

in FIGURE 8. In that figure, l_p, m_c, m_p, θ, x and u represent respectively the pendulum length, cart mass, pendulum mass, pendulum angular position, cart position and horizontal driving force. The nonlinear motion equations are found by means of Lagrangian equations [57], [58], from which the "cyclic" coordinate x can simply be removed to be left with the second-order equation as [57], [59], and:

$$\left(1 - \frac{3m_p}{4(m_p+m_c)}\,cos^2\theta\right)\ddot{\theta} + \frac{3m_p}{8(m_p+m_c)}\dot{\theta}^2\,sin(2\theta) - \frac{3g}{2l_p}\,sin\,\theta - \frac{3u(t)}{2l_p(m_p+m_c)}\,cos\theta = 0 \tag{40}$$

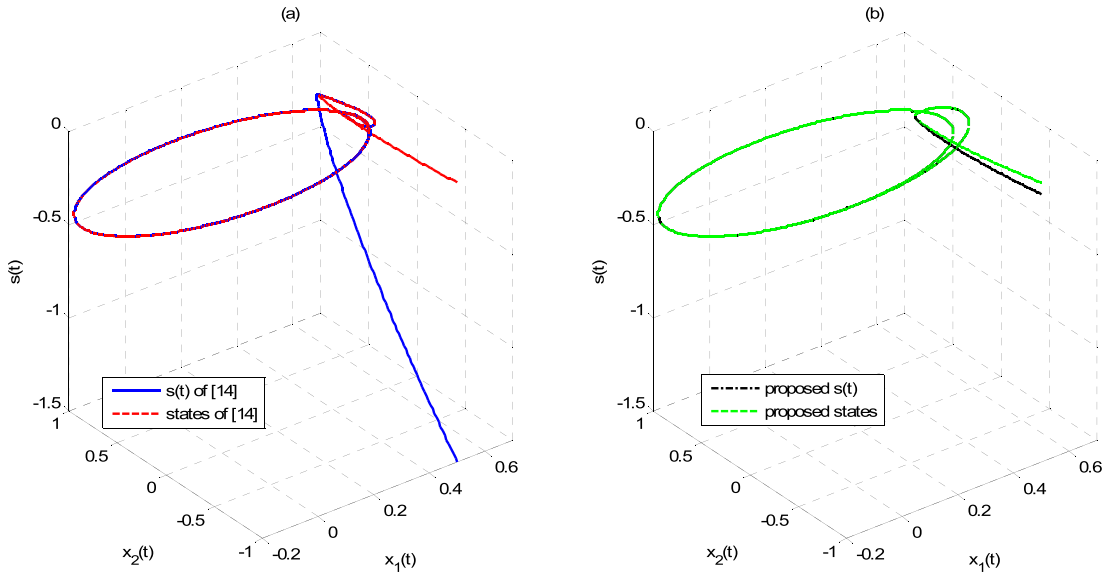

FIGURE 13. Phase plot of the states and sliding surfaces; (a) method of [14], (b) proposed method.

or equivalently:

$$l_p\left(\frac{4}{3}(m_p+m_c)-m_p\,cos^2\theta\right)\ddot{\theta} = 2g(m_p+m_c)\,sin\,\theta - \frac{1}{2}m_p l_p\dot{\theta}^2\,sin(2\theta)+2u(t)\,cos\,\theta. \quad (41)$$

Defining $x_1 = \theta$ and $x_2 = \dot{\theta}$, yields the following state-space presentation [60]:

$$\dot{x}_1 = x_2,$$
$$\dot{x}_2 = \frac{2g(m_c+m_p)\,sin(x_1)-m_p l_p x_2^2\,sin(x_1)\,cos(x_1)}{l_p\left(\frac{4}{3}(m_c+m_p)-m_p\,cos^2(x_1)\right)} + \frac{2\,cos(x_1)}{l_p\left(\frac{4}{3}(m_c+m_p)-m_p\,cos^2(x_1)\right)}u(t)+d(x,t), \quad (42)$$

where x_1, x_2, g are the pendulum angular position, pendulum angular velocity and gravitational acceleration, respectively. The parameters of the inverted pendulum are set as: $l_p = 0.5m$, $m_p = 0.1kg$, $m_c = 1kg$, $g = 9.8m/s^2$. The disturbance is given as: $d(x,t) = 0.3\,cos(x_1) + 0.2\,cos(\pi t) + 0.1\,sin(1.5t)u$. Using (1) and (42), the nonlinear functions are specified as: $f(x,t) = \frac{2g(m_c+m_p)\,sin(x_1)-m_p l_p x_2^2\,sin(x_1)\,cos(x_1)}{l_p\left(\frac{4}{3}(m_c+m_p)-m_p\,cos^2(x_1)\right)}$ and $b(x,t) = \frac{2\,cos(x_1)}{l_p\left(\frac{4}{3}(m_c+m_p)-m_p\,cos^2(x_1)\right)}$.

The initial states are given by: $x(0) = \begin{bmatrix}0.5 & -1\end{bmatrix}^T$ and the desired trajectory is chosen as: $x_d(t) = 0.5\,sin(t)$. The constant parameters are chosen by trial and error as $\gamma_1 = \frac{1}{3}$, $\gamma_2 = 0.5$, $\varepsilon_1 = 0.04$, $\varepsilon_2 = 0.07$, $\rho_1 = 1.1$, $\rho_2 = 1.05$, $c_1 = 0.5$, $c_2 = 1.2$, $\psi = 7$, $\gamma = 0.5$, $\kappa = 15$, and $\eta = 0.3$. The trajectories of the angular position and angular velocity are depicted in FIGURE 9 and FIGURE 10, respectively.

TABLE 2. Performance indices (IAE, ITAE, ISV) of the pendulum system.

	IAE		*ITAE*		*ISV*
	e_1	e_2	e_1	e_2	
proposed method	0.2862	0.5026	0.1145	0.3035	2.153
method in [14]	0.3242	0.5014	0.2034	0.3278	2.281

It can be inferred from these figures that the position and velocity states suitably track the reference signals using the proposed method. The control input of the system is displayed in FIGURE 11, which shows smooth and fchattering-free dynamics. From FIGURE 12, it can be observed that the planned sliding surface is smooth and approaches to zero quickly. FIGURE 13 demonstrates the phase plots of the states and sliding surfaces. It can be obviously seen that the proposed sliding surface and system states converge to the equilibrium faster than those of the method of [14]. All these figures verify that the offered control technique has much better robust performance compared to the method of [14]. The IAE, ITAE and ISV comparative results are given in Table 2. It can be observed from Table 2 that the performance indices values are much less for the proposed control technique in comparison with the other method. Then, by comparing the simulation results, one can conclude that the tracking performance of the suggested control method is superior to that of the method of [14].

Two other simulations are executed to study the robustness of the proposed method to various external disturbances. For this purpose, the exterior disturbances are set to triangle and square waveforms with $d(t) = \begin{cases}-0.5\,(t-1)\,, 0 \le t < 2\\ 0.5\,(t-3)\,, 2 \le t < 4\end{cases}$

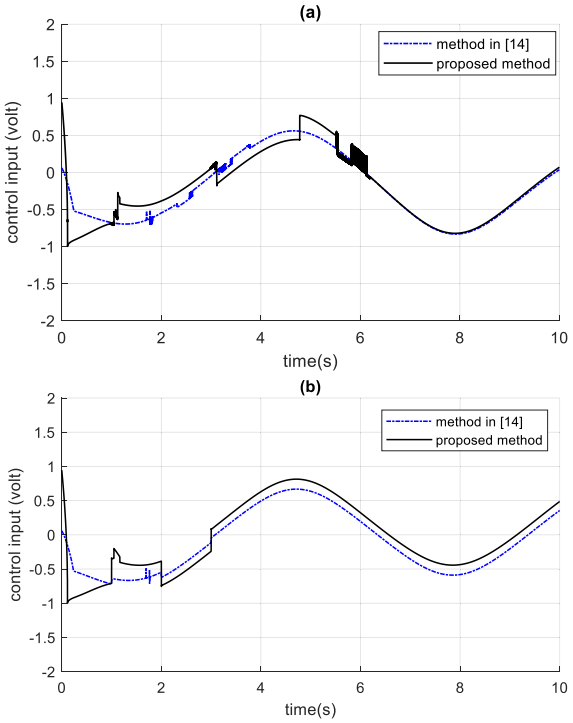

FIGURE 14. Control signals in the presence of (a) triangle wave disturbance, (b) square wave disturbance.

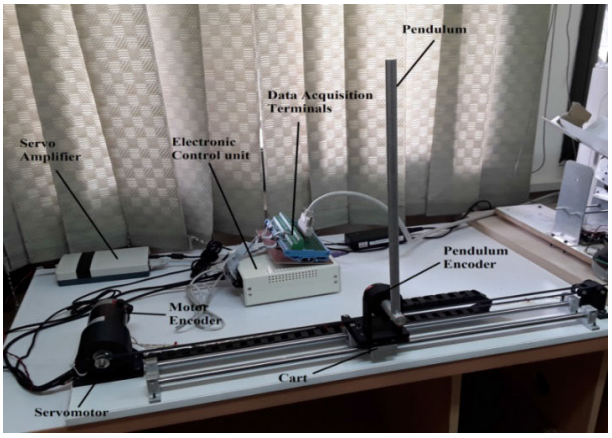

FIGURE 15. Built in cart-inverted pendulum system.

and $d(t) = \begin{cases} 0.5, 0 \leq t < 1 \\ -0.5, 1 \leq t < 2 \end{cases}$, correspondingly. Simulation results are obtained without retuning the gains of the control signal. In both cases, the time responses of the angular positions, angular velocities and sliding surfaces are similar to the results for the sinusoidal disturbance $d(x,t) = 0.3\ cos(x_1) + 0.2\ cos(\pi t) + 0.1\ sin(1.5t)u$, and thus are not repeated here. Time trajectories of the control signals for both cases are given in FIGURE 14, which demonstrates the chattering problem in the new cases.

An experimental verification of the proposed approach is carried out via MATLAB® Simulink® and Real-Time

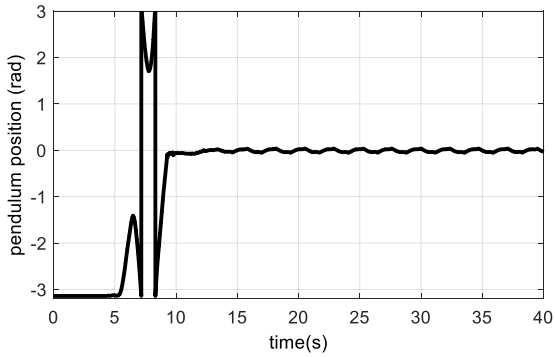

FIGURE 16. Time response of the pendulum angle.

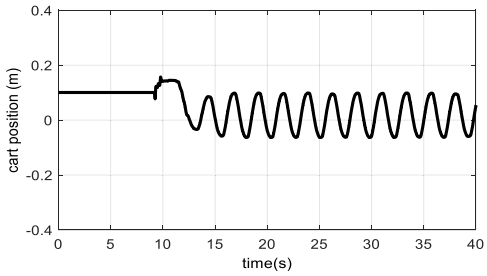

FIGURE 17. Time response of the cart position.

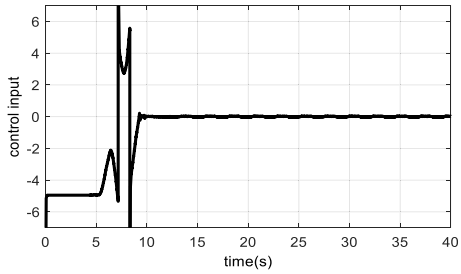

FIGURE 18. Control input of built in system.

toolboxes. We execute experiments on the practical cart-inverted pendulum system depicted in FIGURE 15. The angular position of the pendulum and the linear position of the cart are measured using two E40S encoders by Autonics Company. The employed card in this practical system is the PCI-1751, which is connected to the computer via D/A and A/D converters. The obtained pendulum's angular position and cart's linear position are shown in FIGURE 16 and FIGURE 17, respectively. The position of the inverted pendulum is changes from π to 0, and stabilizes around the equilibrium. These experimental results prove the performance of the proposed approach. The control signal is illustrated in FIGURE 18.

The above practical results confirm the good tracking performance and effectiveness of the proposed control scheme.

V. CONCLUSION

This paper proposed an adaptive non-singular fast terminal sliding mode control (FTSMC) with integral surface for the

finite time tracking control of nonlinear systems with external disturbances. It main objective is to establish strong robust performance, fast finite time convergence and chattering-free dynamics. The proposed approach substitutes the signum function with a bipolar function with tunable coefficients and derives an appropriate adaptive parameter-tuning law to tackle the unknown bounded disturbances and alleviate the undesired chattering problem. It also does not require the time-derivative of the fractional power terms in the controller, thereby eschewing the singularity problem. Implementation of the proposed approach to a VDP circuit and an inverted pendulum confirmed its good tracking performance. Additionally, a comparison study to the approach proposed in [14] highlighted its superior performance and dynamic response. Our future work will focus on augmenting the proposed approach with continuous finite time convergence differentiators and implementing the proposed design for chaos suppression, chaotic synchronization and filter design.

REFERENCES

[1] J. Fei and H. Wang, "Recurrent neural network fractional-order sliding mode control of dynamic systems," *J. Franklin Inst.*, vol. 357, no. 8, pp. 4574–4591, May 2020.

[2] J. Yang, S. Li, and X. Yu, "Sliding-mode control for systems with mismatched uncertainties via a disturbance observer," *IEEE Trans. Ind. Electron.*, vol. 60, no. 1, pp. 160–169, Jan. 2013.

[3] L. Dong and W. C. Tang, "Adaptive backstepping sliding mode control of flexible ball screw drives with time-varying parametric uncertainties and disturbances," *ISA Trans.*, vol. 53, no. 1, pp. 110–116, 2014.

[4] Q.-D. Zhu, R.-T. Yu, G.-H. Xia, and Z.-L. Liu, "Sliding-mode robust tracking control for underactuated surface vessels with parameter uncertainties and external disturbances," *Control theory Appl.*, vol. 29, no. 7, pp. 959–964, 2012.

[5] H. Pan, G. Zhang, H. Ouyang, and L. Mei, "Novel fixed-time nonsingular fast terminal sliding mode control for second-order uncertain systems based on adaptive disturbance observer," *IEEE Access*, vol. 8, pp. 126615–126627, 2020.

[6] G. Zhang, P. He, H. Li, Y. Tang, Z. Li, X.-Z. Xiong, W. Wei, and Y. Li, "Sliding mode control: An incremental perspective," *IEEE Access*, vol. 8, pp. 20108–20117, 2020.

[7] V. Utkin, A. Poznyak, Y. Orlov, and A. Polyakov, "Conventional and high order sliding mode control," *J. Franklin Inst.*, vol. 357, no. 15, pp. 10244–10261, Oct. 2020.

[8] S. Bayhan and H. Komurcugil, "Sliding-mode control strategy for three-phase three-level T-type rectifiers with DC capacitor voltage balancing," *IEEE Access*, vol. 8, pp. 64555–64564, 2020.

[9] W. Qin, "Unit sliding mode control for disturbed crowd dynamics system based on integral barrier Lyapunov function," *IEEE Access*, vol. 8, pp. 91257–91264, 2020.

[10] J. Wu and Y. Lu, "Adaptive backstepping sliding mode control for boost converter with constant power load," *IEEE Access*, vol. 7, pp. 50797–50807, 2019.

[11] J. Katebi, M. Shoaei-parchin, M. Shariati, N. T. Trung, and M. Khorami, "Developed comparative analysis of metaheuristic optimization algorithms for optimal active control of structures," *Eng. Comput.*, vol. 36, pp. 1–20, Jun. 2019.

[12] W. Jawaada, M. S. M. Noorani, and M. M. Al-sawalha, "Active sliding mode control antisynchronization of chaotic systems with uncertainties and external disturbances," *J. Appl. Math.*, vol. 2012, Apr. 2012, Art. no. 293709.

[13] S.-H. Chang, P.-Y. Chen, Y.-H. Ting, and S.-W. Hung, "Robust current control-based sliding mode control with simple uncertainties estimation in permanent magnet synchronous motor drive systems," *IET Electr. Power Appl.*, vol. 4, no. 6, pp. 441–450, 2010.

[14] Y.-C. Huang and T.-H.-S. Li, "Design of an adaptive terminal sliding-function controller for nonlinear multivariable systems," *Int. J. Robust Nonlinear Control*, vol. 25, no. 6, pp. 937–948, Apr. 2015.

[15] M. R. Soltanpour, M. H. Khooban, and M. Soltani, "Robust fuzzy sliding mode control for tracking the robot manipulator in joint space and in presence of uncertainties," *Robotica*, vol. 32, no. 3, pp. 433–446, May 2014.

[16] K. Mei and S. Ding, "Second-order sliding mode controller design subject to an upper-triangular structure," *IEEE Trans. Syst., Man, Cybern. Syst.*, vol. 51, no. 1, pp. 497–507, Jan. 2021.

[17] K. Rabiei and K. Parand, "Collocation method to solve inequality-constrained optimal control problems of arbitrary order," *Eng. Comput.*, vol. 36, no. 1, pp. 115–125, Jan. 2020.

[18] Z. Yang, Q. Ding, X. Sun, H. Zhu, and C. Lu, "Fractional-order sliding mode control for a bearingless induction motor based on improved load torque observer," *J. Franklin Inst.*, vol. 358, no. 7, pp. 3701–3725, May 2021.

[19] I.-C. Baik, K.-H. Kim, and M.-J. Youn, "Robust nonlinear speed control of PM synchronous motor using boundary layer integral sliding mode control technique," *IEEE Trans. Control Syst. Technol.*, vol. 8, no. 1, pp. 47–54, Jan. 2000.

[20] S.-L. Shi, J.-X. Li, and Y.-M. Fang, "Extended-state-observer-based chattering free sliding mode control for nonlinear systems with mismatched disturbance," *IEEE Access*, vol. 6, pp. 22952–22957, Apr. 2018.

[21] Y. Zhang, R. Li, T. Xue, Z. Liu, and Z. Yao, "An analysis of the stability and chattering reduction of high-order sliding mode tracking control for a hypersonic vehicle," *Inf. Sci.*, vol. 348, pp. 25–48, Jun. 2016.

[22] K. Mei and S. Ding, "HOSM controller design with asymmetric output constraints," *Sci. China Inf. Sci.*, vol. 65, no. 8, Aug. 2022.

[23] V. Nguyen, C. Lin, S. Su, and Q. Tran, "Adaptive chattering free neural network based sliding mode control for trajectory tracking of redundant parallel manipulators," *Asian J. Control*, vol. 21, no. 2, pp. 908–923, Mar. 2019.

[24] J. A. González, A. Barreiro, S. Dormido, and A. Baños, "Nonlinear adaptive sliding mode control with fast non-overshooting responses and chattering avoidance," *J. Franklin Inst.*, vol. 354, no. 7, pp. 2788–2815, May 2017.

[25] S. Mondal and C. Mahanta, "Chattering free adaptive multivariable sliding mode controller for systems with matched and mismatched uncertainty," *ISA Trans.*, vol. 52, no. 3, pp. 335–341, May 2013.

[26] X. Zhang, X. Liu, and Q. Zhu, "Adaptive chatter free sliding mode control for a class of uncertain chaotic systems," *Appl. Math. Comput.*, vol. 232, pp. 431–435, Apr. 2014.

[27] M. P. Aghababa and M. E. Akbari, "A chattering-free robust adaptive sliding mode controller for synchronization of two different chaotic systems with unknown uncertainties and external disturbances," *Appl. Math. Comput.*, vol. 218, no. 9, pp. 5757–5768, 2012.

[28] J.-L. Chang and J.-C. Tsai, "Dynamic output feedback sliding mode controller design for chattering avoidance," *J. Mar. Sci. Technol.*, vol. 22, no. 3, pp. 277–284, 2014.

[29] H. F. Ho, Y. K. Wong, and A. B. Rad, "Adaptive fuzzy sliding mode control with chattering elimination for nonlinear SISO systems," *Simul. Model. Pract. Theory*, vol. 17, no. 7, pp. 1199–1210, Aug. 2009.

[30] M. Kale, M. Karabacak, W. Kruschel, F. Kilic, and P. Zacharias, "Chattering free robust control of LCL filter based shunt active power filter using adaptive second order sliding mode and resonant controllers," *Int. J. Electr. Power Energy Syst.*, vol. 76, pp. 174–184, Mar. 2016.

[31] Y. Xu, F. Jia, C. Ma, J. Mao, and S. Zhang, "Chatter free sliding mode control of a chaotic coal mine power grid with small energy inputs," *Int. J. Mining Sci. Technol.*, vol. 22, no. 4, pp. 477–481, Jul. 2012.

[32] Q. Xu, "Precision motion control of piezoelectric nanopositioning stage with chattering-free adaptive sliding mode control," *IEEE Trans. Autom. Sci. Eng.*, vol. 14, no. 1, pp. 238–248, Jan. 2017.

[33] D. W. H. Q. Ding, S. G. Lee, and H. Bae, "Suppression of chaotic behaviors in a complex biological system by disturbance observer-based derivative-integral terminal sliding mode," *IEEE/CAA J. Autom. Sinica*, vol. 7, no. 1, pp. 126–135, Jan. 2020.

[34] D. Qian and G. Fan, "Neural-network-based terminal sliding mode control for frequency stabilization of renewable power systems," *IEEE/CAA J. Automatica Sinica*, vol. 5, no. 3, pp. 706–717, May 2018.

[35] H. Pan and W. Sun, "Nonlinear output feedback finite-time control for vehicle active suspension systems," *IEEE Trans. Ind. Informat.*, vol. 15, no. 4, pp. 2073–2082, Apr. 2019.

[36] H. Pan, X. Jing, W. Sun, and H. Gao, "A bioinspired dynamics-based adaptive tracking control for nonlinear suspension systems," *IEEE Trans. Control Syst. Technol.*, vol. 26, no. 3, pp. 903–914, May 2018.
[37] Y. Feng, X. Yu, and Z. Man, "Non-singular terminal sliding mode control of rigid manipulators," *Automatica*, vol. 38, no. 12, pp. 2159–2167, 2002.
[38] H. Li, L. Dou, and Z. Su, "Adaptive nonsingular fast terminal sliding mode control for electromechanical actuator," *Int. J. Syst. Sci.*, vol. 44, no. 3, pp. 401–415, Mar. 2013.
[39] C. Pukdeboon and P. Siricharuanun, "Nonsingular terminal sliding mode based finite-time control for spacecraft attitude tracking," *Int. J. Control Autom. Syst.*, vol. 12, no. 3, pp. 530–540, Jun. 2014.
[40] Z. Wang, Y. Su, and L. Zhang, "A new nonsingular terminal sliding mode control for rigid spacecraft attitude tracking," *ASME J. Dyn. Syst., Meas., Control.*, vol. 140, no. 5, May 2018, Art. no. 051006, doi: 10.1115/1.4038094.
[41] J. Geng, Y. Sheng, and X. Liu, "Time-varying nonsingular terminal sliding mode control for robot manipulators," *Trans. Inst. Meas. Control*, vol. 36, no. 5, pp. 604–617, Jul. 2014.
[42] M. Van, S. S. Ge, and H. Ren, "Finite time fault tolerant control for robot manipulators using time delay estimation and continuous nonsingular fast terminal sliding mode control," *IEEE Trans. Cybern.*, vol. 47, no. 7, pp. 1681–1693, Jul. 2017.
[43] C. Han, L. Yang, and J. Zhang, "Adaptive nonsingular fast terminal sliding mode control for aircraft with center of gravity variations," *Proc. Inst. Mech. Eng. G, J. Aerosp. Eng.*, vol. 229, no. 1, pp. 4–9, 2015.
[44] X. Chang, L. Liu, W. Ding, D. Liang, C. Liu, H. Wang, and X. Zhao, "Novel nonsingular fast terminal sliding mode control for a PMSM chaotic system with extended state observer and tracking differentiator," *J. Vibrat. Control*, vol. 23, no. 15, pp. 2478–2493, Aug. 2017.
[45] L. Xin, Q. Wang, and Y. Li, "A new fast nonsingular terminal sliding mode control for a class of second-order uncertain systems," *Math. Problems Eng.*, vol. 2016, Dec. 2016, Art. no. 1743861.
[46] R. R. Nair and L. Behera, "Robust adaptive gain nonsingular fast terminal sliding mode control for spacecraft formation flying," in *Proc. 54th IEEE Conf. Decis. Control (CDC)*, Dec. 2015, pp. 5314–5319.
[47] C. Jing, H. Xu, X. Niu, and X. Song, "Adaptive nonsingular terminal sliding mode control for attitude tracking of spacecraft with actuator faults," *IEEE Access*, vol. 7, pp. 31485–31493, 2019.
[48] S. Yi and J. Zhai, "Adaptive second-order fast nonsingular terminal sliding mode control for robotic manipulators," *ISA Trans.*, vol. 90, pp. 41–51, Jul. 2019.
[49] M. T. Frye, S. Ding, C. Qian, and S. Li, "Fast convergent observer design for output feedback stabilisation of a planar vertical takeoff and landing aircraft," *IET Control Theory Appl.*, vol. 4, no. 4, pp. 690–700, Apr. 2010.
[50] A. Isidori, *Nonlinear Control Systems*. New York, NY, USA: Springer-Verlag, 1995, doi: 10.1007/978-1-84628-615-5.
[51] P. Li, J. Ma, Z. Zheng, and L. Geng, "Fast nonsingular integral terminal sliding mode control for nonlinear dynamical systems," in *Proc. 53rd IEEE Conf. Decis. Control*, Dec. 2014, pp. 4739–4746.
[52] A. Loría, E. Panteley, and H. Nijmeijer, "A remark on passivity-based and discontinuous control of uncertain nonlinear systems," *Automatica*, vol. 37, no. 9, pp. 1481–1487, Sep. 2001.
[53] M. Chen, Q.-X. Wu, and R.-X. Cui, "Terminal sliding mode tracking control for a class of SISO uncertain nonlinear systems," *ISA Trans.*, vol. 52, no. 2, pp. 198–206, Mar. 2013.
[54] J.-X. Xu, Y.-J. Pan, and T.-H. Lee, "Sliding mode control with closed-loop filtering architecture for a class of nonlinear systems," *IEEE Trans. Circuits Syst. II, Exp. Briefs*, vol. 51, no. 4, pp. 168–173, Apr. 2004.
[55] I. Hassanzade and S. Mobayen, "PSO-based controller design for rotary inverted pendulum system," *J. Appl. Sci.*, vol. 8, no. 16, pp. 2907–2912, Aug. 2008.
[56] I. Hassanzadeh and S. Mobayen, "Controller design for rotary inverted pendulum system using evolutionary algorithms," *Math. Problems Eng.*, vol. 2011, Oct. 2011, Art. no. 572424.
[57] G. Stépán and L. Kollár, "Balancing with reflex delay," *Math. Comput. Model.*, vol. 31, nos. 4–5, pp. 199–205, Feb. 2000.
[58] J.-J. E. Slotine and W. Li, *Applied Nonlinear Control*, no. 1. Englewood Cliffs, NJ, USA: Prentice-Hall, 1991.
[59] J. Sieber and B. Krauskopf, "Complex balancing motions of an inverted pendulum subject to delayed feedback control," *Phys. D, Nonlinear Phenomena*, vol. 197, nos. 3–4, pp. 332–345, Oct. 2004.
[60] J. Liu and F. Sun, "A novel dynamic terminal sliding mode control of uncertain nonlinear systems," *J. Control Theory Appl.*, vol. 5, no. 2, pp. 189–193, 2007.

KHALID A. ALATTAS (Member, IEEE) received the B.Sc. degree in computer science from King Abdulaziz University, Saudi Arabia, the M.Sc. degree in telecommunication networks from New York University, NY, USA, and the M.Sc. and Ph.D. degrees in computer science from the University of Louisiana at Lafayette, Lafayette, USA. He is currently an Assistant Professor with the College of Computer Science and Engineering, University of Jeddah, Saudi Arabia. He serves as a reviewer for many international journals. His research interests include networks, machine learning, and data analytics.

SALEH MOBAYEN (Senior Member, IEEE) received the B.Sc. and M.Sc. degrees in control engineering from the University of Tabriz, Tabriz, Iran, in 2007 and 2009, respectively, and the Ph.D. degree in control engineering from Tarbiat Modares University, Tehran, Iran, in January 2013. Since December 2018, he has been an Associate Professor of control engineering with the Department of Electrical Engineering, University of Zanjan. He currently cooperates with the National Yunlin University of Science and Technology. He has published many articles in national and international journals. He serves as a member of program committee for IEEE conferences.

SAMI UD DIN (Member, IEEE) received the B.Sc. degree in electrical engineering from the Federal Urdu University of Arts, Science & Technology, Islamabad, Pakistan, in 2009, the M.Sc. degree in electronics engineering from Muhammad Ali Jinnah University, Islamabad, in 2012, and the Ph.D. degree in electrical engineering (control systems) from the Capital University of Science & Technology, Islamabad, in 2019. He was with the Department of Electrical Engineering, The University of Lahore, Islamabad, untill October 2019, as an Assistant Professor. He is currently with the Department of Electrical Engineering, Namal Institute Mianwali, Mianwali, Pakistan. His research interests include nonlinear control, robust control, sliding mode control, underactuated robots, and chaotic systems.

JIHAD H. ASAD received the B.Sc. and M.Sc. degrees in physics from An-Najah National University, Palestine, in 1995 and 1998, respectively, and the Ph.D. degree in theoretical physics from The University of Jordan, Amman, Jordan, in 2004. He is currently working as a Full Professor of theoretical physics with Palestine Technical University, Palestine. He is a member of the Institute of Physics (IOP). He serves as a member of program committee for several national and international conferences and finally, he serves as a reviewer for many international journals.

AFEF FEKIH (Senior Member, IEEE) received the B.Sc., M.Sc. and Ph.D. degrees in electrical engineering from the National Engineering School of Tunis, Tunisia, in 1995, 1998, and 2002, respectively. She is currently a Full Professor with the Department of Electrical and Computer Engineering and the Chevron/BORSF Professor in engineering with the University of Louisiana at Lafayette, Lafayette, USA. She has authored or coauthored more than 200 publications in international journals, chapters, and conference proceedings. Her research interests include control theory and applications, including nonlinear and robust control, optimal control, fault tolerant control with applications to power systems, wind turbines, and unmanned vehicles and automotive engines. She is a member of the Editorial Board of IEEE Conference on Control Technology and Applications, IEEE TRANSACTIONS ON EDUCATION, and IFAC TC on Power and Energy Systems.

WUDHICHAI ASSAWINCHAICHOTE (Member, IEEE) received the B.Sc. degree (Hons.) in electrical engineering from Assumption University, Bangkok, Thailand, in 1994, the M.E. degree in electrical engineering from Pennsylvania State University (Main Campus), PA, USA, in 1997, and the Ph.D. degree in electrical engineering from The University of Auckland, New Zealand, in 2004. He is currently an Associate Professor with the Department of Electronic and Telecommunication Engineering, King Mongkut's University of Technology Thonburi, Bangkok. He has published a research monograph and more than 20 research articles in international refereed journals indexed by SCI/SCIE. His research interests include fuzzy control, robust control, optimal control, systems and control theory, and computational intelligence. He currently serves as an Associate Editor for *International Journal of Innovative Computing, Information and Control*.

MAI THE VU received the B.Sc. degree in naval architecture and marine engineering from the Ho Chi Minh City University of Technology, Vietnam, in 2013, and the Ph.D. degree from the Department of Convergence Study on the Ocean Science and Technology, Korea Maritime & Ocean University, South Korea, in 2019. He is currently an Assistant Professor with the Department of Unmanned Vehicle Engineering, Sejong University, South Korea. His research interests include nonlinear control, underwater vehicles and robotics, multi-body dynamic modeling, obstacle avoidance, and intelligent navigation.